Current Biology, Vol. 15, 2271–2278, December 20, 2005, ©2005 Elsevier Ltd All rights reserved. DOI 10.1016/j.cub.2005.10.037

Report

Slit and Robo Control Cardiac Cell Polarity and Morphogenesis

Li Qian,[1,2] Jiandong Liu,[1,2] and Rolf Bodmer[1,*]
[1] The Burnham Institute
Center for Neuroscienes and Aging
10901 North Torrey Pines Road
La Jolla, California 92037
[2] Graduate Program in Molecular, Cellular and Developmental Biology
University of Michigan
Ann Arbor, Michigan 48109

Summary

Basic aspects of heart morphogenesis involving migration, cell polarization, tissue alignment, and lumen formation may be conserved between *Drosophila* and humans, but little is known about the mechanisms that orchestrate the assembly of the heart tube in either organism. The extracellular-matrix molecule Slit and its Robo-family receptors are conserved regulators of axonal guidance. Here, we report a novel role of the *Drosophila slit*, *robo*, and *robo2* genes in heart morphogenesis. Slit and Robo proteins specifically accumulate at the dorsal midline between the bilateral myocardial progenitors forming a linear tube. Manipulation of Slit localization or its overexpression causes disruption in heart tube alignment and assembly, and *slit*-deficient hearts show disruptions in cell-polarity marker localization within the myocardium. Similar phenotypes are observed when Robo and Robo2 are manipulated. Rescue experiments suggest that Slit is secreted from the myocardial progenitors and that Robo and Robo2 act in myocardial and pericardial cells, respectively. Genetic interactions suggest a cardiac morphogenesis network involving Slit/Robo, cell-polarity proteins, and other membrane-associated proteins. We conclude that Slit and Robo proteins contribute significantly to *Drosophila* heart morphogenesis by guiding heart cell alignment and adhesion and/or by inhibiting cell mixing between the bilateral compartments of heart cell progenitors and ensuring proper polarity of the myocardial epithelium.

Results and Discussion

Myocardial and Pericardial Cells Misalign in *slit* and *robo* Mutants

Drosophila has become an excellent model system to unravel basic genetic mechanisms of heart development that are relevant to vertebrates despite their more complex heart structures, as is exemplified by the transcription factor Tinman [1–4]. Furthermore, early embryonic events of heart formation are remarkably similar between *Drosophila* and vertebrates, in that two bilaterally symmetrical strips of precardiac mesoderm fuse as a linear tube at the ventral or dorsal midline in both systems [1, 5]. Although there is much interest in understanding the basis of heart-tube assembly [6], little is known about the underlying molecular-genetic mechanisms that orchestrate this and other morphogenetic processes. *Drosophila* Slit, an EGF- and LRR-containing secreted protein, is expressed in the heart [7, 8], and thus may participate in heart morphogenesis. Slit functions as a repulsive ligand for the Roundabout (Robo) family of receptors in the CNS and acts both attractively and repulsively in trachea and somatic muscles [9–13]. In vertebrates, there are three *slit* and three *robo* genes [14–18]. Among them, Slit3 is expressed prominently in the developing atrial walls of the murine heart. A Slit3 gene-trap mouse exhibits abnormal heart formation, including an apparent enlargement of the right ventricle [19]. Whether or not this heart defect is secondary to other embryonic defects is not known, nor is the genetic or cellular mechanism underlying this phenotype. It is also not known which of the Robo receptors and other Slit proteins play a role in heart development.

To assess the role of Slit in *Drosophila* heart, we analyzed *slit* null-mutant embryos ($slit^2$) by labeling the heart with antibodies against Dmef2, a muscle-specific transcription factor expressed in all myocardial and other muscle cells [20, 21]. When the bilateral rows of myocardial progenitors have reached the dorsal midline, they fail to align properly in *slit* mutants compared to wild-type (Figures 1A, 1B, and 1J). A similar phenotype is observed in *robo,robo2* double-mutant embryos (Figures 1D and 1J). In contrast, only subtle alignment defects are found in *robo* or *robo2* single mutants (Figures 1C and 1J). Unlike *robo* or *robo2*, *robo3* mutants in combination with *robo* or *robo2* do not cause additional heart defects (data not shown), and thus *robo3* is unlikely involved in cardiac development. Similar alignment phenotypes were observed with nmr^{H15}lacZ reporter, a marker for myocardial nuclei [22–24], in *slit* mutants (Figures 1E–1I). Although the dorsal migration of the myocardial progenitors does not seem to be affected, their highly regular arrangement is already perturbed before they reach the midline, as manifested in gaps and double rows (Figures 1E and 1F). Visualization of the pericardial cells with Zfh-1 [25] shows that their alignment with the myocardial cells is also perturbed in *slit-robo* mutants (Figures S1A–S1E in the Supplemental Data available with this article online). At stage 16, two types of phenotypes can be distinguished: Type I consists of irregular cell arrangements (Figure 1H), and type II, in addition, has large gaps (Figure 1I). These two types of phenotypes are found in roughly equal proportion in *slit* and *robo,robo2* double mutants (Figure 1J). These defects are unlikely caused by abnormalities in cardiac lineage specification or in ectodermal epithelium formation during dorsal closure (Figures S1F, S1G, and S2; data not shown).

*Correspondence: rolf@burnham.org

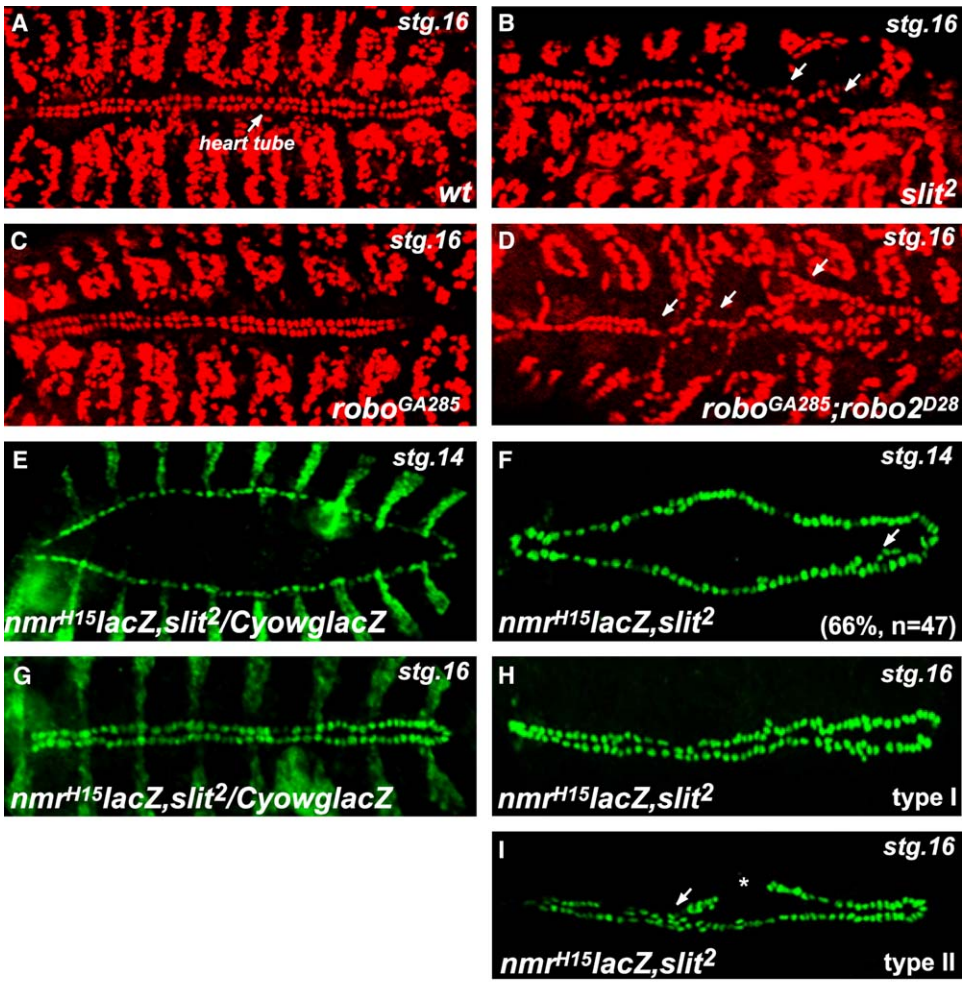

J	*slit*^{2}	*robo*^{GA285}	*robo2*^{D28}	*robo*^{GA285}, *robo2*^{D28}
type I	51%	6%	18%	44%
type II	49%	0	0	56%
n	67	34	50	27

Figure 1. Cardiac Morphogenesis Defects in *slit*/*robo* Mutants

(A) Wild-type Dmef2-labeled myocardial cell (MC) nuclei of the heart tube (arrow) at stage 16.

(B) Loss of *slit* results in abnormalities of heart morphology, as indicated by misaligned MCs (arrows).

(C) *robo* single mutants exhibit no defects detectable by Dmef2-labeled MC nuclei.

(D) Double mutants for *robo* and *robo2* show severe MC misalignment including gaps, intercalation, and double rows (arrows), as in *slit* mutants (B).

(E–I) *nmr*^{H15}lacZ reporter expression in MCs of the heart tube. (E–F) Before cardiac cells reach the dorsal midline, only mild alignment defects are observed in *slit* mutant hearts (arrow in [F]) compared to heterozygous sibling controls (E). (G–I) After reaching dorsal midline, *slit* mutants exhibit two types of MC misalignments: Type I consist of irregularities in the MC rows (H), and type II, in addition, has gaps (asterisk) and triple lines of MCs (arrow) (I).

(J) Quantification for percentage of misaligned heart tube in *slit*; *robo*; *robo2*; and *robo,robo2* mutants at stage 16.

Expression and Specificity of Slit and Robo in the Developing Heart

Given the cardiac abnormalities of *slit* and *robo* mutants, we examined the expression pattern of *slit* and its receptors in the developing heart. Slit protein is first detected in the heart at stage 14, uniformly distributed within the myocardial cytoplasm (Figures 2A, 2A′, and 2I). As the bilateral rows of cardiac progenitors align at the dorsal midline, Slit accumulates at the contact sites between them (Figure 2B, 2B′, and 2I). Like Slit, Robo initially displays a similarly uniform cortical localization within myocardial cells (Figures 2C, 2C′, and 2I). Once they reach the midline, Robo enriches strongly at the dorsal (apical) surface of the cell (Figures 2E and 2E′ and insets). In contrast, Robo2 is present in pericardial cells located ventrally to the myocardial cells (Figures 2D, 2D′, 2H, and

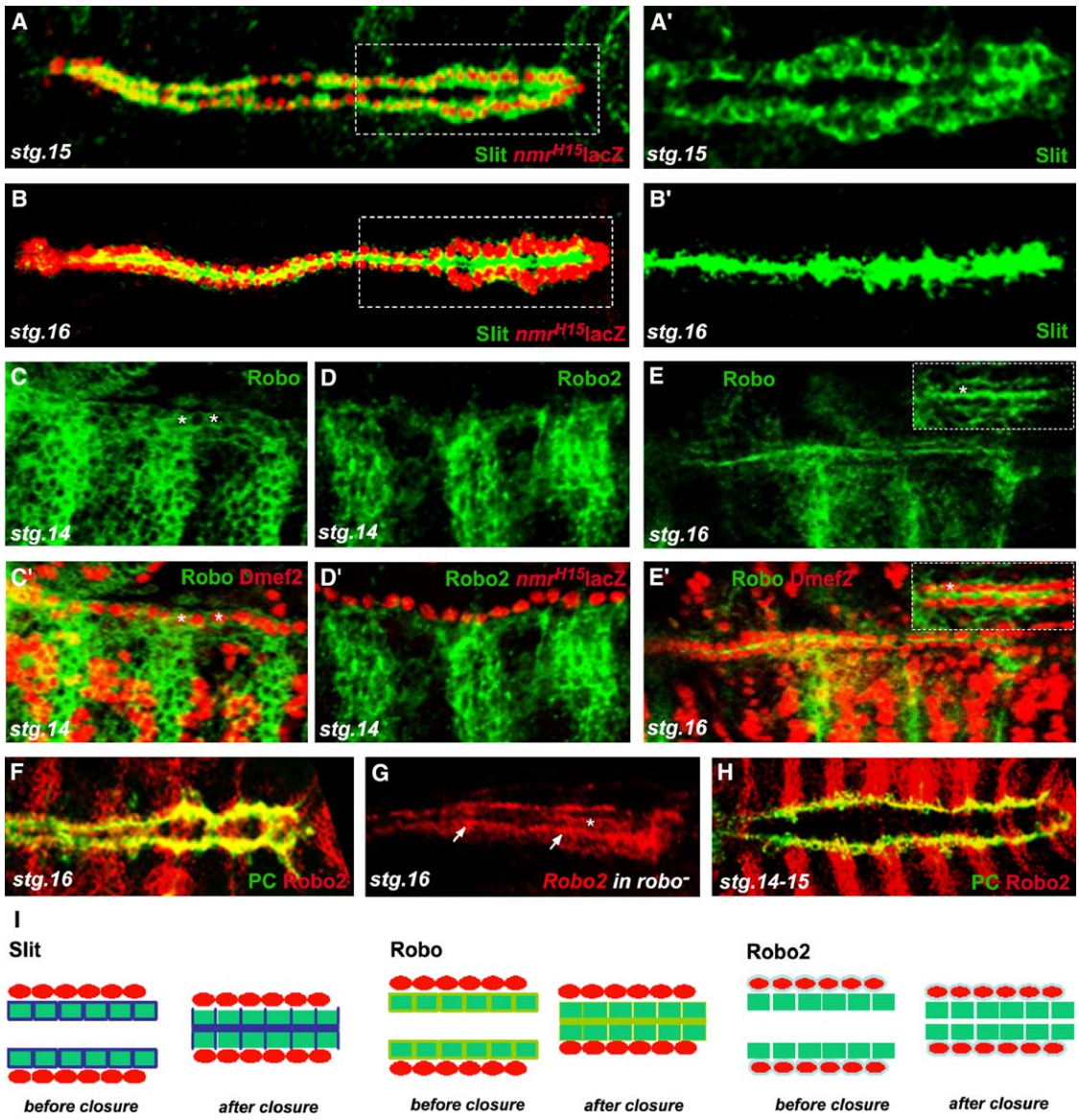

Figure 2. Slit/Robo Localization in *Drosophila* Hearts

(A and A′) Before dorsal closure, Slit protein is present throughout nmr^{H15}lacZ-labeled MCs (except the nuclei).

(B and B′) At stage 16, Slit is highly accumulated at the dorsal midline where bilateral MC rows contact each other. ([A′] and [B′] are magnifications of dotted regions in [A] and [B]).

(C and C′) Expression of Robo in MCs before they reach the dorsal midline. Note the distribution of Robo throughout the membranes of Dmef2-labeled MCs (asterisks indicate the same nuclei in [C] and [C′]).

(D and D′) Robo2 expression is in cells located ventrally to the nmr^{H15}lacZ-labeled MCs.

(E and E′ and insets) Stage 16 embryos show that Robo protein is highly enriched apically between the MC rows at the dorsal midline. Asterisks mark the same MC nucleus in [E] and [E′] insets.

(F and H) Robo2 double-labeling with Pericardin (labeling the surface of pericardial cells, PCs) suggests that Robo2 is expressed in PCs. Note that unlike Slit and Robo, Robo2 does not accumulate at the midline at stage 16 (F). However, in *robo* single mutants, Robo2 is ectopically expressed in MCs (asterisk) and accumulates at midline (arrows) (G).

(I) Cartoon illustrating the dynamic localization of Slit, Robo, and Robo2 in *Drosophila* heart before and after MC alignment. Green rectangles show myocardial cells, red ovals show pericardial cells, blue lines show Slit protein, green lines show Robo protein, and light-green circles show Robo2 protein.

2I). Unlike Slit and Robo, Robo2 does not accumulate at the midline but remains in pericardial cells (Figures 2F and 2I). In *robo* mutants, however, *robo2* is ectopically expressed in myocardial cells and enriches at the dorsal midline (Figure 2G), similar to Robo in wild-type embryos. Thus, *robo2* apparently compensates for a myocardial loss-of-*robo* function, and this compensation is consistent with their redundant requirement in cardiac morphogenesis (see Figure 1J).

Although Slit and Robo are indeed expressed in the heart, indirect effects cannot be ruled out because they function in multiple tissues [10, 26–28]. To address whether *slit*/*robo* acts autonomously within the heart, we performed tissue- and cell-type-specific rescue

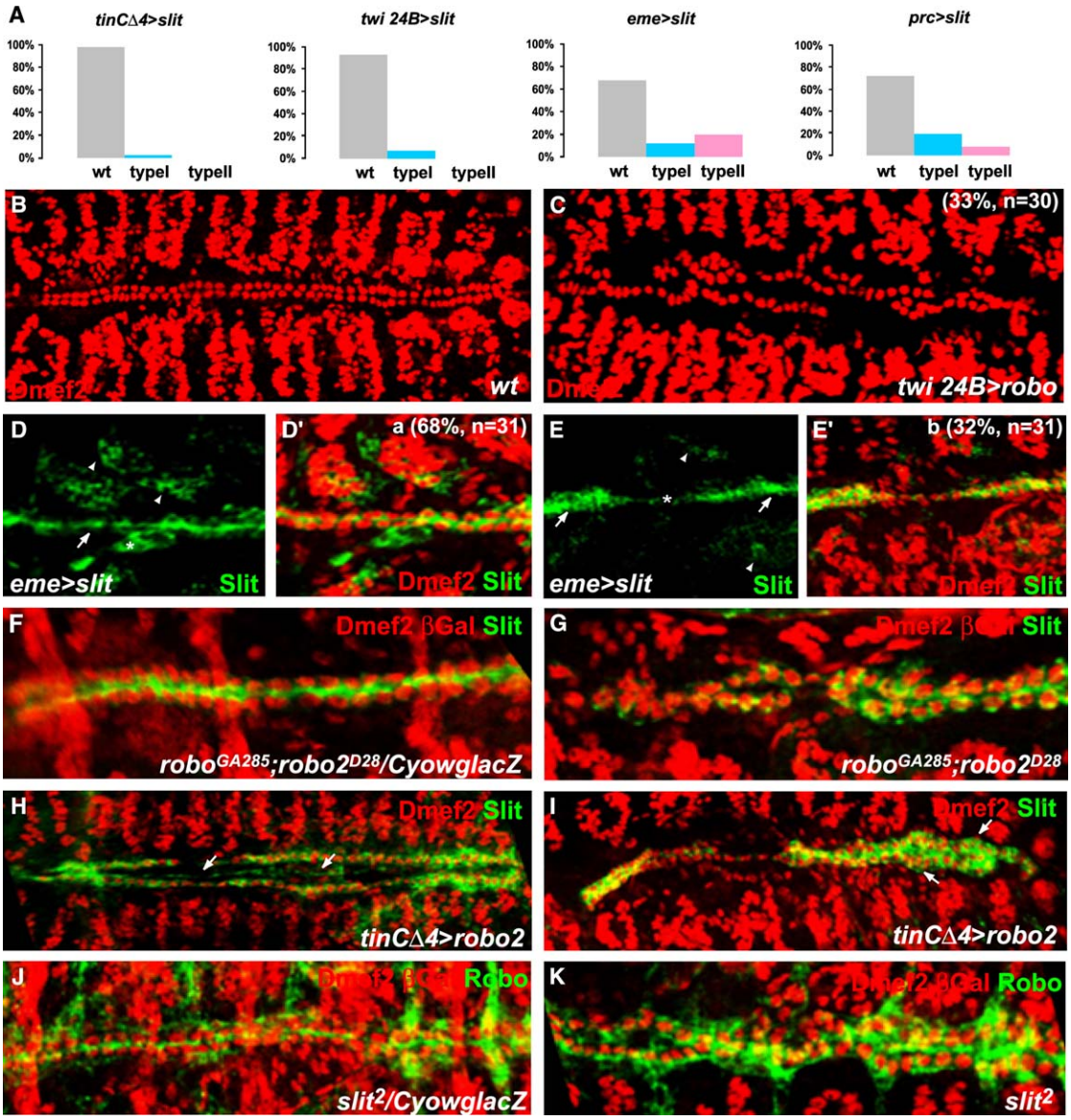

Figure 3. Altered Slit Localization at the Dorsal Midline Causes Defective Cardiac Morphology

(A) Histogram of wild-type, type I, and type II heart phenotypes (see Figures 1H and 1I) in *tinCΔ4>slit*, *twi 24B>slit*, *eme>slit*, and *prc>slit* embryos. Sample size is 30–50.

(B and C) Overexpression of robo in the mesoderm. Note the severe alignment defects in the heart.

(D–E′) Misexpression of *slit* in PCs (asterisk) and DA muscles (arrowheads) with eme-Gal4 gives rise to a misaligned myocardium (some ectopic Slit is not in focus). Note normal Slit accumulation at the dorsal midline of unaffected hearts (arrow in [D]) and mispatterned (arrows in [E]) or missing Slit protein (asterisk in [E]) in defective hearts (E′).

(F and G) Slit is not concentrated at the dorsal midline in *robo,robo2* mutants (G), compared to heterozygous sibling controls (F).

(H) Slit accumulates prematurely at the dorsal midline (arrows) when *robo2* is misexpressed in MCs (stage 15).

(I) Slit midline localization is perturbed when *robo2* is mixexpressed in MCs (stage 16). Note that Slit is distributed throughout the MCs (arrows).

(J and K) In the absence of *slit*, Robo localization in the heart is also disrupted (K), compared to heterozygous sibling controls (J).

experiments. We found that *slit* and *robo* expression within myocardial cells is sufficient to rescue the *slit* and *robo,robo2* phenotype, respectively, in promoting normal heart morphogenesis (Figure S3).

Slit Concentration at the Midline Is Crucial for Myocardial Cell Alignment

Because *slit* and *robo* are expressed at the cardiac midline and are required for heart cell alignment, we wondered if local mislocalization of these proteins also causes cardiac morphogenesis defects. Myocardial-specific (tinCΔ4-driver) or pan-mesodermal (twi24B-driver) overexpression of *slit* does not produce significant cardiac alignment defects or only with low penetrance (7%, n = 32), respectively (Figure 3A), suggesting that augmenting Slit levels in myocardial cells hardly perturbs cardiac cell alignment. Mesodermal *robo* overexpression, however, results in frequent alignment defects (Figure 3C), as does ectopic expression of *slit* in pericardial cells (Figures 3A, 3E, and 3E′). Interestingly,

in those embryos that exhibit virtually normal cardiac alignment, Slit accumulates continuously at the cardiac midline (Figures 3D and 3D′). In contrast, the embryos with significant abnormalities also mispattern Slit (Figures 3E and 3E′). Precise midline accumulation of Slit thus seems to be critical to correctly align and assemble the heart tube.

Because we observed similar cardiac misalignment defects in *robo,robo2* as in *slit* mutants (Figures 1B and 1D), we wondered whether Slit accumulation is affected in *robo,robo2* embryos. Indeed, without *robo* and *robo2*, Slit no longer concentrates evenly at the contact point between the myocardial cells (Figures 3F and 3G). Thus, loss of Robo receptors compromises Slit accumulation at the dorsal midline. When *robo2* is misexpressed in myocardial cells by using tinCΔ4-Gal4, we observed a premature midline accumulation of Slit (Figure 3H), and upon contact of the bilateral cardiac rows, Slit no longer concentrates at the cardiac midline (Figure 3I). It may be also that misexpressed Robo2 receptors trap Slit in the cytoplasm and prevent its proper secretion. When Robo or Robo2 is expressed throughout the mesoderm, the Slit pattern is also severely disrupted (data not shown), and the heart tube is frequently misaligned (Figure 3C). Because pan-mesodermal expression of *slit* is of little consequence, it may be that the localization of Robo is crucial for Slit accumulation at the midline. However, *slit* mutants do not exhibit correct Robo patterning either (Figures 3J and 3K), thus implying that *slit* is necessary but not sufficient (or instructive) for Robo localization.

slit Is Required for Apical-Lateral Polarity Acquisition of the Heart Tube

Previous reports suggest a role of cardiac cell-polarity acquisition in heart morphogenesis [22, 29, 30]. Failure to correctly polarize the cardiac epithelium may result in misalignments that are independent of the earlier specification and differentiation events [22]. To study the polarity of the cardiac epithelium in *slit* mutants, we first examined Dlg, which localizes to the basolateral sides of myocardial epithelium before contact of the bilateral rows is established (Figures 4A and 4A′), and to the apical-lateral sides after contact (Figures 4C and 4C′) [22]. Unlike in the dorsal ectoderm (Figure S2), cardiac Dlg localization is severely compromised in *slit* mutants as the bilateral heart primordia come in contact (Figures 4D and 4D′). Because a polarity phenotype is manifest only upon heart-tube assembly (Figures 4B, 4B′, 4 D, and 4D′), *slit* does not appear to be required for guiding the cardiac epithelium to the dorsal midline or for initiating its polarity before contact, but rather for correctly switching its polarity from basal-lateral to apical-lateral (diagram in Figures 4A and 4C). Examination of myocardial polarity of *slit* mutants with two other basal-lateral to apical-lateral makers, α-Spectrin and Armadillo, shows defects similar to those observed with Dlg (data not shown). In addition, we examined the transmembrane protein Toll, which is present on the apical-lateral surface of myocardial cells during, but not before, the cardiac alignment process (Figure 4E) [31, 32]. As with Dlg, α-Spectrin, and Armadillo, Toll protein is no longer restricted to the apical-lateral sides of the myocardial cells in *slit* mutants (Figures 4E and 4F). Toll mislocalization can be rescued by expressing a *slit* transgene in the hearts of *slit* mutants (Figures S3N and S3N′). The disruption in apical-lateral patterning of all cell-polarity makers we examined suggests an important function of *slit* in polarity acquisition and maintenance. Consistent with this conclusion is the accumulation of Slit and Robo at the dorsal myocardial midline (Figures 2B and 2E), which potentially mediates the switch in myocardial cell polarity as a prerequisite for heart-tube formation.

In contrast to the apical-lateral localization of the previous markers, Dystroglycan (Dg) is heavily enriched at both apical and basal sides of myocardial membrane, but is excluded laterally [22]. Interestingly, in *slit* mutant hearts, polarized Dg localization does not seem to be significantly altered despite the severe cardiac morphogenetic defects (Figures 4G and 4H). This is in contrast to Tbx20 *neuromancer (nmr)* mutants, in which myocardial polarity is also disrupted, including Dg localization [22].

Genetic Interaction between *slit* and Cell-Polarity Genes

We anticipate that there are numerous molecules involved in generating or maintaining cardiac cell polarity in conjunction with *slit/robo* during heart morphogenesis, but mutants of some key factors may be early lethal or have pleiotropic effects. Thus, we chose to study genetic interactions between cell-polarity genes and *slit* in relation to cardiac morphogenesis. For this purpose, we made various transheterozygous combinations between *slit* and polarity genes that are expressed in the heart [22, 30], including *dg*, *dlg*, and *shortgun* (*shg*, encoding E-cadherin, and mutants previously shown to have cardiac defects [30]). As single heterozygotes, they do not have detectable heart abnormalities, but removal of one copy of *slit* and *dg*, *shg*, or *dlg* results in defective cardiac morphogenesis (Table 1). In contrast, *crumbs(crb)* does not interact with *slit* in the heart, which is consistent with the lack of (polarized) Crb localization in the cardiac epithelium (Figure S2). Taken together, these observations suggest that *slit* and cell-polarity genes cooperate in aligning the myocardium. Slit/Robo localization is also perturbed in *nmr* mutants (Figure S4), suggesting that Tbx20-mediated transcriptional activities also influence Slit/Robo localization in the heart.

Possible Autocrine Mechanisms of Robo/Slit Function in Heart Formation

Slit is well known as a repellent signal that emanates from the CNS midline and patterns axon tracks, muscles, and tracheal branches [10–13, 26, 27]. Slit can also act as an attractant [26, 27], but in all cases seems to be secreted from another cell type than its receptors. In contrast, during *Drosophila* heart morphogenesis, both Slit and Robo originate from the same cells, i.e., from the cardiomyocytes as they align at the dorsal midline. During this apparently autocrine process, Slit ligands and Robo receptors relocalize from the myocardial circumference to accumulate between the bilateral cell rows (Figure 2), mediating aligned adhesion between these rows. It is presently unknown how Slit and Robo relocalize to the apical side of the heart, but this process is likely to require the function of cell-polarity

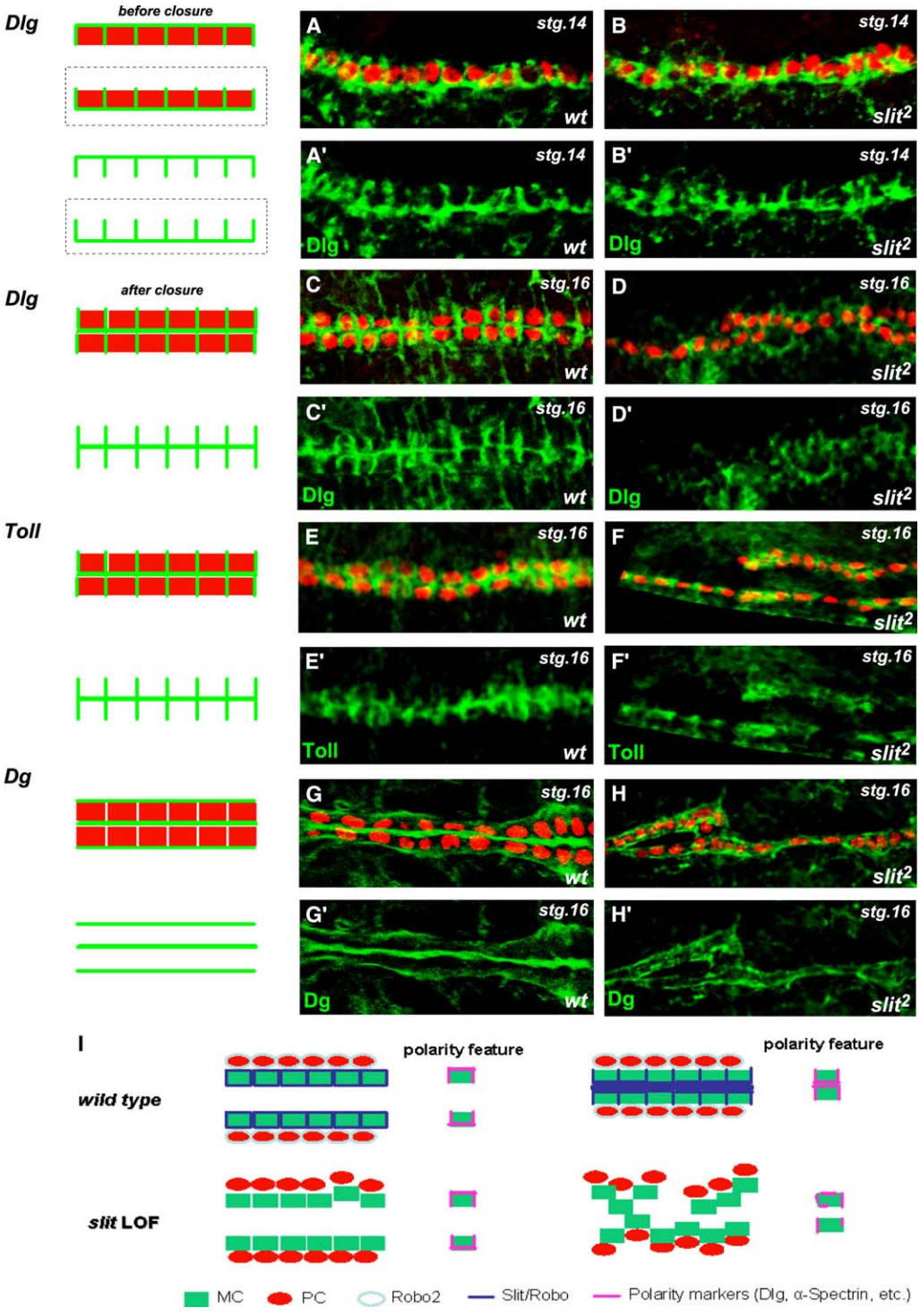

Figure 4. Epithelial-Polarity Features of a *slit*-Depleted Myocardium

nmr^{H15}lacZ-labeled MC nuclei are in red, and cell-polarity markers are in green, Dlg (A–D′), Toll (E–F′), Dg (G–H′).

(A and B) Before closure, Dlg is distributed at basal and lateral sides of myocardial cells (A and A′), and this pattern is not affected in *slit* mutant MCs (B and B′).

(C–D′) As the MCs come in contact, Dlg is redistributed to the apical(dorsal)-lateral sides of the MCs (C and C′), and this pattern is no longer maintained in the absence of *slit* (D and D′).

(E–F′) Toll shows a similar pattern of subcellular localization as Dlg (E and E′), and its deposition is compromised in *slit* mutants as well (F and F′).

(G–H′) Dg labels the apical and basal sides of the MCs but is excluded from the lateral sides (G and G′). Although MC alignment is defective, Dg still localizes to apical and basal membranes (H and H′).

(I) Diagram summarizing the localization of Slit, Robo, Robo2, and polarity markers in the heart before and after the bilateral MC rows reach the dorsal midline in wild-type and *slit* loss-of-function (LOF) mutants.

Table 1. Quantification of Heart Morphogenesis Defect in *slit* and Cell-Polarity Gene Mutants

	Normal in Cardiac Cell Alignment	Defective in Cardiac Cell Alignment	Total Number
slit^{2}/Cyo-wglacZ	100%	0%	30
slit^{2}	0%	100%	67
dg^{248}/Cyo-enlacZ	100%	0%	53
dg^{248}	100%	0%	48
Df(2R)JP6Dg/Cyo-enlacZ	100%	0%	31
Df(2R)JP6Dg	4%	96%	25
slit^{2},+/+, dg^{248}	62%	38%	26
slit^{2},+/+, Df(2R)JP6Dg	53%	47%	51
dlg^{1}/FM7-GFP	100%	0%	38
dlg^{1}	100%	0%	18
dlg^{1}/+(Y), slit^{2}/+	59%	41%	34
shg^{2}/Cyo-wglacZ	100%	0%	49
shg^{2}	48%	52%	27
slit^{2},+/+, shg^{2}	70%	30%	30
crb^{11A2}/TM3-ftzlacZ	100%	0%	32
slit^{2},+/+, crb^{11A2}	96%	4%	45

genes, such as *dlg* and others, that genetically interact with *slit* (Table 1) and are repolarized themselves (Figure 4). It may also be that a Slit molecule can bind Robo receptors on both sides of the midline, perhaps in a cooperative manner, which would then lead to a progressive accumulation of both receptors and ligands at the midline and thus to a precise alignment of the bilateral rows. This is reminiscent of the attractive Robo-Slit interaction during muscle patterning: Robo is made in the muscles of adjacent segments and accumulates at the Slit-secreting muscle-attachment sites between the segments [27]. Regardless of the difference in cellular origin, Slit may bind Robo receptors across the segment boundary, just as we propose Slit may interact with Robo proteins across the midline between the myocardial rows. Such a Robo-Slit-mediated adhesion process is also consistent with the observed myocardial-epithelium repolarization, which would bring the bilateral rows of cells in close proximity. In *slit* mutants, morphogenetic defects not only include failed alignments but also double alignments and intercalation. Thus, mutant cardiomyocytes often reach the midline and get in close proximity with the contralateral side but then seem to intermix. Therefore, we propose that Robo-Slit act as heterophilic cell-adhesion molecules mediating coordinated stereotyped alignment as well as inhibiting cell mixing. In conclusion, we propose that Slit/Robo proteins act in concert with cell-polarity genes in guiding and maintaining myocardial (and pericardial) cell alignment, which is likely a prerequisite for later morphogenetic events, such as formation of a continuous cardiac lumen precisely at the position of Slit localization.

Experimental Procedures

Drosophila *Stocks*

The following mutants were used: [*slit^{2}/Cyo-wglacZ*] [10]; [*yw;b,pr,pk,cn,robo^{GA285}/Cyo,wg-lacZ*], [*yw;robo2^{1}/Cyo,wg-lacZ*], and [*yw;robo2^{D28},robo^{GA285}/Cyo,wg-lacZ*] [11]; [*nmr1^{614},b,cn;ry^{506}*] [22]; [*dlg^{1}/FM7*] [33]; [*dg^{248}/Cyo,en-lacZ*] and [*Df(2R)JP6Dg/Cyo, en-lacZ*] [34]; [*shg^{2}/Cyo*] [30]; and [*crb^{11A2}/TM3*] [35].

Overexpression of transgenes was achieved by using the UAS-Gal4 system [36]. The following drivers were used: *twi*-Gal4 (twi>), *24B*-Gal4 (24B>; [36]), the double combination *twi*-Gal4;*24B*-Gal4 (twi24B>; pan-mesodermal expression. twi-Gal4 drives expression in all mesoderm cells from stage 9 onward until stage 12 and 24B-Gal4 in the cardiac and somatic mesoderm from stage 10/11 on; data now shown), tinCΔ4-Gal4 (in *tinman*-expressing myocardial cells; [37]), eme-Gal4 (in *even skipped*-expressing pericardial cells and DA muscles; [38]), 69B-Gal4 (ectodermal expression; [36]), elav-Gal4 (pan-neuronal expression), and prc-Gal4 (pericardial expression).

The following UAS lines were used: UAS-*slit* [10], UAS-*robo,* UAS-*robo2* [11], UAS-*nmr2*RNAi, and UAS-nmr2 [22]. The following combined genotypes were made: [*slit^{2},nmr^{H15}lacZ/Cyo, wg-lacZ*] [*slit^{2}/Cyo,wg-lacZ;UAS-slit*], [*slit^{2}/Cyo,wg-lacZ;24B-Gal4*], [*slit^{2}/Cyo,wg-lacZ;tinCΔ4-Gal4*], [*slit^{2}/Cyo,wg-lacZ;eme-Gal4*], [*slit^{2}/Cyo,wg-lacZ;69B-Gal4*], [*slit^{2}/Cyo,wg-lacZ;prc-Gal4/TM3,ftz-lacZ*], [*robo2^{D28},robo^{GA285}/Cyo,wg-lacZ;UAS-robo*], [*robo2^{D28},robo^{GA285}/Cyo,wg-lacZ;UAS-robo2*], [*robo2^{D28},robo^{GA285}/Cyo,wg-lacZ;24B-Gal4*], [*robo2^{D28},robo^{GA285}/Cyo,wg-lacZ;*tinCΔ4-Gal4], [*robo2^{D28}, robo^{GA285}/Cyo,wg-lacZ; elav-Gal4*], and [*robo2^{D28},robo^{GA285}/Cyo, wg-lacZ;prc-Gal4/TM3,ftz-lacZ*].

Immunohistochemistry

Antibody staining was performed as described [38]. Cy3- or FITC-conjugated secondary antibodies (Jackson Labs) were used for fluorescent confocal microscopy. All the secondary antibodies were used at 1:200. Embryos with fluorescent staining were mounted in VectaShield (Vector Laboratories) and preparations were analyzed with Zeiss LSM510 and Biorad MRC-1024MP confocal microscopes.

The following primary antibodies were used in this study: rabbit anti-Robo2 [11]; rabbit anti-Toll [31]; mouse anti-Lbe, 1:40 [39]; rabbit anti-Eve, 1:300 [40]; rabbit anti-Tinman, 1:1000 [41]; rabbit anti-β-Galactosidase, 1:2000 (Cappel); mouse anti-β-Galactosidase, 1:500 (Sigma); rabbit anti-DMef2, 1:2000 [21]; and rabbit anti-Dystroglycan (DG) 1:2000 [34]. The following primary antibodies used are all from Hybridoma Bank, University of Iowa: mouse anti-Slit (1:500); mouse anti-Robo (1:200); mouse anti-Robo3 (1:200); mouse anti-Crumbs (1:100); mouse anti-Disc large (Dlg) 1:500; mouse anti-Armadillo (Arm) 1:500; and mouse anti-α-Spectrin (Spec) 1:100.

Supplemental Data

Supplemental Data include four figures and are available with this article online at: http://www.current-biology.com/cgi/content/full/15/24/2271/DC1/.

Acknowledgments

We thank Barry Dickson, Greg Bashaw, Steven Wasserman, Hannele Ruohola-Baker, Manfred Frasch, Christophe Jagla, Michel Sémériva, and Stephane Zaffran; the Bloomington stock center; and Developmental Studies Hybridoma Bank for sending fly stocks and antibodies. L.Q. is supported by a predoctoral fellowship from the American Heart Association. This work was funded by grants from the National Institutes of Health (NHLBI) to R.B.

Received: August 29, 2005
Revised: October 11, 2005
Accepted: October 14, 2005
Published: December 19, 2005

References

1. Bodmer, R. (1995). Heart development in *Drosophila* and its relationship to vertebrate systems. Trends Cardiovasc. Med. *5*, 21–27.
2. Cripps, R.M., and Olson, E. (2002). Control of cardiac development by an evolutionarily conserved transcriptional network. Dev. Biol. *246*, 14–28.
3. Bodmer, R. (1993). The gene tinman is required for specification of the heart and visceral muscles in *Drosophila*. Development *118*, 719–729.
4. Azpiazu, N., and Frasch, M. (1993). *tinman* and *bagpipe*: Two homeobox genes that determine cell fates in the dorsal mesoderm of *Drosophila*. Genes Dev. *7*, 1325–1340.

5. Bodmer, R., and Frasch, M. (1999). Genetic determination of *Drosophila* heart development. In Heart Development. N. Rosenthal, and R. Harvey, eds. (San Diego: Academic Press). pp. 65–90.
6. Moorman, A.F., and Christoffels, V.M. (2003). Cardiac chamber formation: Development, genes, and evolution. Physiol. Rev. *83*, 1223–1267.
7. Rothberg, J.M., Hartley, D.A., Walther, Z., and Artavanis-Tsakonas, S. (1988). slit: An EGF-homologous locus of *D. Melanogaster* involved in the development of the embryonic central nervous system. Cell *55*, 1047–1059.
8. Rothberg, J.M., Jacobs, J.R., Goodman, C.S., and Artavanis-Tsakonas, S. (1990). slit: An extracellular protein necessary for development of midline glia and commissural axon pathways contains both EGF and LRR domains. Genes Dev. *4*, 2169–2187.
9. Brose, K., Bland, K.S., Wang, K.H., Arnott, D., Henzel, W., Goodman, C.S., Tessier-Lavigne, M., and Kidd, T. (1999). Slit proteins bind robo receptors and have an evolutionarily conserved role in repulsive axon guidance. Cell *96*, 795–806.
10. Kidd, T., Bland, K.S., and Goodman, C.S. (1999). Slit is the midline repellent for the Robo receptor in Drosophila. Cell *96*, 785–794.
11. Rajagopalan, S., Nicolas, E., Vivancos, V., Berger, J., and Dickson, B.J. (2000). Crossing the midline: Roles and regulation of robo receptors. Neuron *28*, 767–777.
12. Simpson, J.H., Bland, K.S., Fetter, R.D., and Goodman, C.S. (2000a). Short-range and long-range guidance by Slit and its Robo receptors: A combinatorial code of Robo receptors controls lateral position. Cell *103*, 1019–1032.
13. Simpson, J.H., Kidd, T., Bland, K.S., and Goodman, C.S. (2000b). Short-range and long-range guidance by Slit and its Robo receptors: Robo and Robo2 play distinct roles in midline guidance. Neuron *28*, 753–766.
14. Nakayama, M., Nakajima, D., Nagase, T., Nomura, N., Seki, N., and Ohara, O. (1998). Identification of high-molecular-weight proteins with multiple EGF-like motifs by motif-trap screening. Genomics *51*, 27–34.
15. Itoh, A., Miyabayashi, T., Ohno, M., and Sakano, S. (1998). Cloning and expressions of three mammalian homologues of Drosophila slit suggest possible roles for Slit in the formation and maintenance of the nervous system. Brain Res. Mol. Brain Res. *62*, 175–186.
16. Holmes, G.P., Negus, K., Burrideg, L., Raman, S., Algar, E., Yamada, T., and Little, M.H. (1998). Distinct but overlapping expression patterns of two vertebrate slit homologs implies functional roles in CNS development and organogenesis. Mech. Dev. *79*, 57–72.
17. Li, H.S., Chen, J.H., Wu, W., Fagaly, T., Zhou, L., Yuan, W., Dupuis, S., Jiang, Z.H., Nash, W., Gick, C., et al. (1999). Vertebrate slit, a secreted ligand for the transmembrane protein roundabout, is a repellent for olfactory bulb axons. Cell *96*, 807–818.
18. Wang, K.H., Brose, K., Arnott, D., Kidd, T., Goodman, C.S., Henzel, W., and Tessier-Lavigne, M. (1999). Biochemical purification of a mammalian slit protein as a positive regulator of sensory axon elongation and branching. Cell *96*, 771–784.
19. Liu, J., Zhang, L., Wang, D., Shen, H., Jiang, M., Mei, P., Hayden, P.S., Sedor, J.R., and Hu, H. (2003). Congenital diaphragmatic hernia, kidney agenesis and cardiac defects associated with Slit3-deficiency in mice. Mech. Dev. *102*, 1059–1070.
20. Bour, B.A., O'Brien, M.A., Lockwood, W.L., Goldstein, E.S., Bodmer, R., Taghert, P.H., Abmayr, S.M., and Nguyen, H.T. (1995). Drosophila MEF2, a transcription factor that is essential for myogenesis. Genes Dev. *9*, 730–741.
21. Lilly, B., Zhao, B., Ranganayakulu, G., Paterson, B.M., Schulz, R.A., and Olson, E.N. (1995). Requirement of MADS domain transcription factor D-MEF2 for muscle formation in *Drosophila*. Science *267*, 688–693.
22. Qian, L., Liu, J., and Bodmer, R. (2005). *Neuromancer (H15/midline)* T-box20-related genes promote cell fate specification and morphogenesis of the *Drosophila* heart. Dev. Biol. *279*, 509–524.
23. Reim, I., Mohler, J.P., and Frasch, M. (2005). Tbx20-related genes, mid and H15, are required for tinman expression, proper patterning, and normal differentiation of cardioblasts in *Drosophila*. Mech. Dev. *122*, 1056–1069.
24. Miskolczi-McCallum, C.M., Scavetta, R.J., Svendsen, P.C., Soanes, K.H., and Brook, W.J. (2005). The *Drosophila melanogaster* T-box genes *midline* and *H15* are conserved regulators of heart development. Dev. Biol. *15*, 459–472.
25. Lai, Z.C., Rushton, E., Bate, M., and Rubin, G.M. (1993). Loss of function of the *Drosophila* zfh-1 gene results in abnormal development of mesodermally derived tissues. Proc. Natl. Acad. Sci. USA *90*, 4122–4126.
26. Englund, C., Steneberg, P., Falileeva, L., Xylourgidis, N., and Samakovlis, C. (2002). Attractive and repulsive functions of Slit are mediated by different receptors in the *Drosophila* trachea. Development *129*, 4941–4951.
27. Kramer, S.G., Kidd, T., Simpson, J.H., and Goodman, C.S. (2001). Switching repulsion to attraction: Changing responses to Slit during transition in mesoderm migration. Science *292*, 737–740.
28. Tayler, T.D., Robichaux, M.B., and Garrity, P.A. (2004). Compartmentalization of visual centers in the *Drosophila* brain requires Slit and Robo proteins. Development *131*, 5935–5945.
29. Fremion, F., Astier, M., Zaffran, S., Guillen, A., Homburger, V., and Semeriva, M. (1999). The heterotrimeric protein Go is required for the formaiton of heart epithelium in *Drosophila*. J. Cell Biol. *145*, 1063–1076.
30. Haag, T.A., Haag, N.P., Lekven, A.C., and Hartenstein, V. (1999). The role of cell adhesion molecules in *Drosophila* heart morphogenesis: Faint sausage, shotgun/DE-cadherin, and laminin A are required for discrete stages in heart development. Dev. Biol. *208*, 56–69.
31. Wang, J., Tao, Y., Reim, I., Gajewski, K., Frasch, M., and Schulz, R.A. (2005). Expression, regulation, and requirement of the Toll transmembrane protein during dorsal vessel formation in *Drosophila melanogaster*. Mol. Cell. Biol. *25*, 4200–4210.
32. Hashimoto, C., Hudson, K.L., and Anderson, K.V. (1988). The *toll* gene of *Drosophila*, required for dorsal-ventral embryonic polarity, appears to encode a transmembrane protein. Cell *52*, 269–279.
33. Abott, L.A., and Natzle, J.E. (1992). Epithelial polarity and cell separation in the neoplastic l(1)dlg-1 mutant of *Drosophila*. Mech. Dev. *37*, 43–56.
34. Deng, W.M., Schneider, M., Frock, R., Castillejo-Lopez, C., Gaman, E.A., Baumgartner, S., and Ruohola-Baker, H. (2003). Dystroglycan is required for polarizing the epithelial cells and the oocyte in *Drosophila*. Development *130*, 173–184.
35. Bilder, D., Schober, M., and Perrimon, N. (2003). Integrated activity of PDZ protein complexes regulates epithelial polarity. Nat. Cell Biol. *5*, 53–58.
36. Brand, A.H., and Perrimon, N. (1993). Targeted gene expression as a means of altering cell fates and generating dominant phenotypes. Development *118*, 401–415.
37. Lo, P.C., and Frasch, M. (2001). A role for the COUP-TF-related gene *seven-up* in the diversification of cardioblast identities in the dorsal vessel of Drosophila. Mech. Dev. *104*, 49–60.
38. Han, Z., Fujioka, M., Su, M., Liu, M., Jaynes, J.B., and Bodmer, R. (2002). Transcriptional integration of competence modulated by mutual repression generates cell-type specificity within the cardiogenic mesoderm. Dev. Biol. *15*, 225–240.
39. Jagla, K., Frasch, M., Jagla, T., Dretzen, G., Bellard, F., and Bellard, M. (1997). ladybird, a new component of the cardiogenic pathway in *Drosophila* required for diversification of heart precursors. Development *124*, 3471–3479.
40. Frasch, M., Hoey, T., Rushlow, C., Doyle, H., and Levine, M. (1987). Characterization and localization of the even-skipped protein of *Drosophila*. EMBO J. *6*, 749–759.
41. Venkatesh, T.V., Park, M., Ocorr, K., Nemaceck, J., Golden, K., Wemple, M., and Bodmer, R. (2000). Cardiac enhancer activity of the homeobox gene tinman depends on CREB consensus binding sites in *Drosophila*. Genesis *26*, 55–66.